

Kunio Kawamoto · Kengo Ishimaru · Yuji Imamura

Reactivity of wood charcoal with ozone

Received: August 18, 2003 / Accepted: November 27, 2003

Abstract We investigated the resistance of wood charcoal against ozone and estimated the half-life of the charcoal in air. The weight of wood charcoal prepared by the carbonization of *Fagus crenata* sawdust at 400°C (C-400) was not affected with up to 8.5% ozone while the charcoal prepared at 1000°C (C-1000) burned with 4.9% ozone. Pores with a diameter of approximately 100–200 nm were observed on the surface of ozone-treated C-1000 by scanning electron microscopy, although no pores were found in ozone-treated C-400. The peak positions of the C1s spectra and the full width at half maximum of X-ray photoelectron spectrum peaks suggest that C-400 has an amorphous structure composed of aliphatic carbons and small aromatic molecules while C-1000 and activated charcoal (AC) are polyaromatic. It is likely that the aromatic layers of C-1000 and AC were destroyed and the edge carbon atoms were removed as CO or CO₂ by ozone oxidation. We estimated the half-life of C-1000 with ozone in air to be about 50 000 years by assuming that the weight of C-1000 decayed exponentially. Thus, it is suggested that wood charcoal is stable on a geological time scale.

Key words Wood charcoal · Ozone · Stability · Oxidation · Half life

K. Kawamoto¹ (✉)
Biological Environment Institute, The General Environmental Technos Co., Ltd., Uji 611-0021, Japan

K. Ishimaru · Y. Imamura
Research Institute for Sustainable Humanosphere, Kyoto University, Uji 611-0011, Japan

Present addresses:

¹Environmental Assessment Department, The General Environmental Technos Co., Ltd., 1-3-5 Azuchimachi, Chuo-ku, Osaka 541-0052, Japan
Tel. +81-6-6263-7407; Fax +81-6-6263-7309
e-mail: kawamoto_kunio@kanso.co.jp

Introduction

Global warming by greenhouse gases has been reported to change the earth's climate.¹ For the purpose of stopping or mitigating global warming, it has been proposed that wood-derived charcoal or carbonized biomass is useful in order to sequester carbon dioxide.^{2,3} The Kansai Electric Power Co. and Kansai Environmental Engineering Center Co. are carrying out a CO₂-sequestration project on an industrial plantation and pulp production enterprise in South Sumatra in Indonesia.⁴ In this project, pulp wood wastes and forest residue are carbonized to charcoal for soil amendment and other applications. It has also been reported that charcoal is useful for soil amendment to propagate symbiotic microorganisms,^{5,6} purification of river water, waste water, and other similar functions,^{7–9} and deodorization against ammonia and trimethylamine.¹⁰ These utilizations are based on charcoal's high stability. There are, however, few reports regarding the chemical degradation of wood charcoal, although observations concerning microbial decay have been reported.³

Many reports have investigated the reactivity of carbon toward ozone,^{11–16} and especially so for activated carbon.^{17–20} Most of these studies, however, focussed on the removal of ozone. Some groups have observed explosion of activated carbon with ozone,^{17,19} but did not elucidate the detailed mechanism of the degradation of activated carbon. Few reports show the degradation of nonactivated wood charcoal in the presence of ozone.

Quantitative assessment of the stability of wood charcoal is necessary when the charcoal is utilized as carbon storage. Carbon credit, under the Kyoto Protocol or the other emissions trading markets, would be derived from charcoal by the sufficient estimation of its degradation characteristics and its ability of carbon storage.

In this study, we investigated the oxidation property of carbonized wood by a surface structural and morphological study, estimated the half-life of wood charcoal with ozone in air, and determined a carbonization temperature to produce wood charcoal suitable for carbon storage.

Table 1. Samples for ozone treatment

Sample name	Sample type	Original material	Carbonizing target temperature (°C)	Size	Manufacturer
C-400	Charcoal	Beech sawdust	400	<2mm	–
C-1000	Charcoal	Beech sawdust	1000	<2mm	–
AC	Activated charcoal	Coconut shells	–	0.5–5 mm	Nacalai Tesque
GR	Graphite	Natural graphite	–	Powder	Nacalai Tesque

Materials and methods

The samples applied for this study are described in Table 1. We prepared two kinds of wood charcoal from the sawdust of *Fagus crenata*. This wood species was selected as a raw material for charcoal, because its high density was suitable for soil amendment and water purification. The sawdust was heated at a heating rate of 5°C/min to target temperatures of 400° and 1000°C in a gas-tight muffle furnace (KBF-668S, Koyo Thermo Systems) with a smoke outlet. The sawdust was maintained at a temperature of 400°C for 24 h (C-400), or kept at 500°C for 6 h and then kept at a target temperature of 1000°C for 6 h (C-1000). Activated charcoal (AC), which has been well investigated regarding its ability to remove ozone, and graphite (GR), which is stable carbon, were used for comparison.

Various concentrations of ozone in oxygen gas were generated with an ozone generator (CFS-1A, Chlorine Engineers) using industrial oxygen gas (Masscoal). The ozone-including oxygen gas was supplied through stainless steel and Teflon tubes to a separable glass flask at 5.0l/min in which 1.0g of the samples (Table 1) in a glass flask (5 cm in diameter) were settled for exposure to ozone. In order to investigate the dependence of the weight decrease of the samples on ozone concentration, they were treated with ozone for 2 h. For estimation of the decline rate of wood charcoal by ozone in air, C-1000 was exposed with ozone for 4 or 5 h. Activated charcoal was also treated with ozone for 2 h for comparison.

After the ozone exposure treatments, weights of the samples were measured, the moisture content was calculated after drying the samples for 1 h at 107°C, and the decreases in the dry weights of the samples caused by ozone exposure were determined.

The surface morphology of the untreated and ozone-treated samples was investigated by scanning electron microscopy (SEM) operating at 10kV (JSM-5310, Jeol).

Carbon, hydrogen, and oxygen contents were analyzed with the samples described in Table 1. The analysis for carbon and hydrogen was carried out using a HCN Coder (MT-700HCN, Yanaco Analytical Instruments), and oxygen was analyzed using an oxygen/nitrogen analyzer (EMGA-620W/A, Horiba). Volatile components were analyzed according to the Japanese Industrial Standard (JIS) M 8812-1993.

A Shimadzu/Kratos AXIS-HS X-ray photoelectron spectrometer (XPS), utilizing Mg K α radiation (1253.6 eV), an output of 150 W, and a system pressure of 1.0 to 2.0 \times

10⁻⁹ torr, was used to analyze the surface chemical structure of the samples. The surface of each sample was scanned ten times. All C1s and O1s spectra were fitted with a data processing program.

The rate constant was calculated from Eq. 1 on the basis of the hypothesis that the weight of charcoal decreased by one order exponentially with the treatment by ozone.

$$\alpha = -\ln(W_t/W_0)/t \quad (1)$$

where α : rate constant (min⁻¹)

t : treatment time by ozone (min)

W_t : weight of the sample after treatment by ozone for t (min)

W_0 : weight of the sample before treatment by ozone

Results and discussion

Weight change of the samples by ozone treatment

The weight change of the samples after treatment for 2 h with up to 8.5% ozone, is shown in Fig. 1. A weight change in C-400 was not observed with up to 8.5% ozone while C-1000 was burned to ash by treatment with 4.9% ozone. The weight of GR was not affected by up to 8.1% ozone. The weight of AC decreased by 11.5% with 2.9% ozone and linearly decreased with up to 7.1% ozone. The AC was burned at 8.5% ozone and a portion of that escaped from the glass flask in which the AC was placed for the ozone treatment.

SEM observation

Figure 2a,b shows SEM micrographs of untreated and ozone-treated C-1000. Pores with a diameter of approximately 100–200 nm were distributed innumerable on the inner surface of the cell wall of the ozone-treated C-1000 (Fig. 2b). Furthermore, small particles with a size of approximately 0.5–1.0 μ m were observed on the cell wall of the ozone-treated C-1000. Figure 2c,d depicts SEM images of C-400. No morphological changes were induced by the ozone treatment. The ozone-treated AC showed the same results as C-1000 (Fig. 2e,f), while the results for GR were similar to those of C-400 (Fig. 2g,h). The results of SEM observations were consistent with the trends in weight loss of the samples caused by ozone treatment.

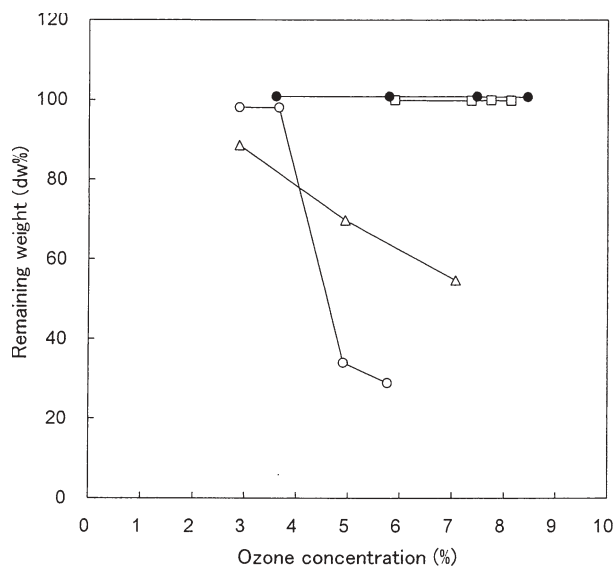


Fig. 1. Weight change of the samples by ozone treatment. *Open circles*, C-1000; *filled circles*, C-400; *triangles*, AC (activated charcoal); *squares*, GR (graphite)

SEM observations (Fig. 2) showed the random distribution of pores and small deposits on the inner surface of the cell wall as a characteristic feature of the ozone-treated samples, which exhibited distinctive weight loss from the ozone treatment (Fig. 1). It is suggested that the microstructure of the ozone-treated sample was more porous than that of the untreated sample. Small deposits on the cell wall were probably carbonaceous components that were generated after dissection of the cell wall during ozone treatment.

Elemental composition and volatile component

Carbon, hydrogen, and oxygen contents in the samples are described in Table 2. The oxygen content of untreated C-400, which had been prepared by carbonization at the lower temperature, was the highest among the untreated samples. The content of volatile components in C-400 was much higher than in C-1000. The weight change of the samples was not affected by the composition of carbon, hydrogen, and oxygen (Fig. 1, Table 2). Therefore, it is suggested that the surface chemical structure of carbon is closely related to the morphological and weight changes of samples caused by ozone treatment.

XPS study

Table 3 shows O1s/C1s ratios from XPS analyses of untreated and ozone-treated samples. The increase in the O1s/C1s ratio means an increase in the amount of oxygen-containing functional groups.²¹ The O1s/C1s ratios of untreated samples displayed different values among them. After ozone treatment, the O1s/C1s ratios in all samples increased noticeably, and were especially large for C-400, C-1000, and AC. The increases in the O1s/C1s ratios after ozone treat-

Table 2. Contents of carbon, hydrogen, oxygen, and volatile components in the samples (wt%)

Sample	C	H	O	Volatile component
C-400	84.3	2.91	5.88	16.3
C-1000	94.8	0.25	1.03	1.3
AC	94.3	0.24	1.64	–
GR	95.2	<0.1	0.26	–

Table 3. Peak position and full width at half maximum (FWHM) of C1s X-ray photoelectron spectra (XPS) and O/C ratios from XPS of carbon materials treated by ozone

Sample	Ozone treatment	O/C ratios	Peak position (eV)	FWHM (eV)
C-400	Untreated	0.30	285.0	2.24
	Treated	0.65	285.3	2.79
C-1000	Untreated	0.29	284.4	1.55
	Treated	0.50	284.6	1.60
AC	Untreated	0.18	284.4	1.36
	Treated	1.27	285.3	2.13
GR	Untreated	0.07	284.4	1.08
	Treated	0.11	284.4	1.08

ment show that oxygen-containing functional groups were added to the edge surfaces of hexagonal carbon layers by oxidation with ozone.

Figure 3 shows high-resolution XPS C1s spectra. A shift in the chemical signal of around 4–7 eV from the main carbon peak (284.4–285.0 eV to 288.5–291.5 eV) was observed in the C1s spectra of C-400, C-1000, and AC after ozone treatment. The chemical shift is caused by carboxyl or ester and carbonate groups and/or chemisorbed CO and CO₂.²² These chemical shifts suggest that carboxyl or ester and carbonate groups were produced by ozone treatment and that a large amount of CO and/or CO₂ gases were chemically adsorbed to the edge of hexagonal carbon layers or into the pores of C-1000 and AC. This was probably due to the distraction of aromatic layers and removal of the edge carbon atoms such as CO or CO₂ by ozone oxidation. Chemical signals induced by potassium were observed at around 296 eV and 293 eV only with C-1000 (Fig. 3).

Peak positions of the C1s spectra of untreated and ozone-treated samples are shown in Table 3. The peak position of untreated C-400 is 285.0 eV, which means that C-400 was composed of aliphatic and small aromatic molecules with a layer size of less than 2.2 nm.^{23,24} On the other hand, a peak position of 284.4 eV for C-1000 and AC means that these carbon materials have a polyaromatic carbon structure.^{25,26} After ozone treatment, the peak positions of the C1s spectra of ozone-treated samples except GR shifted to a higher binding energy. This shift was remarkable for AC. It is suggested that the carbon structure of ozone-treated samples, except GR, suffered some damage by oxidation.²⁷

The C1s line shape parameter full width at half maximum (FWHM) decreases systematically with the increasing polyaromatic character of carbon materials.^{29,30} The FWHM

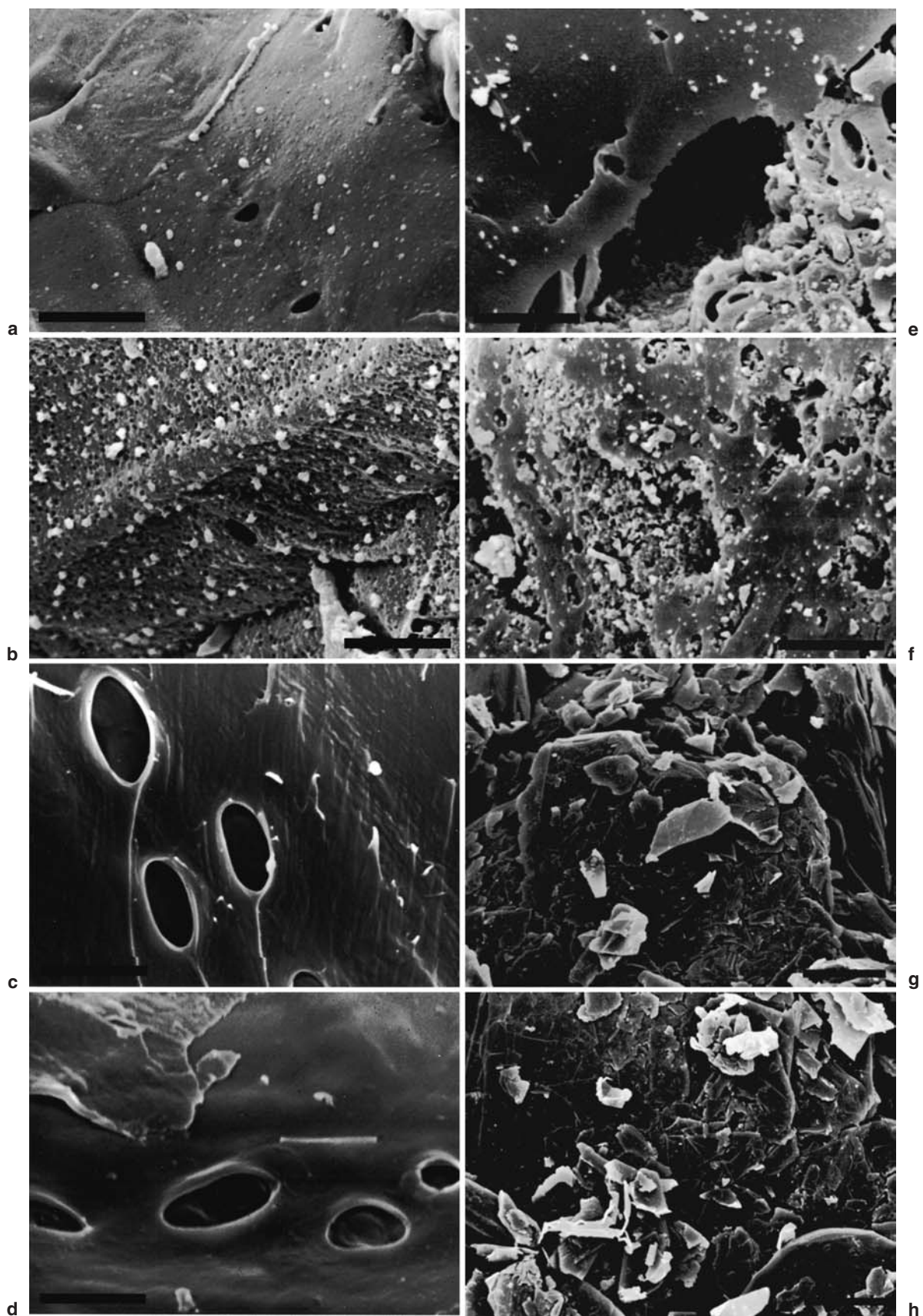


Fig. 2a-h. Scanning electron microscopy (SEM) micrographs of the samples untreated and treated with ozone. **a** C-1000 untreated; **b** C-1000 treated with 3.8% ozone for 4h; **c** C-400 untreated; **d** C-400

treated with 7.3% ozone for 2h; **e** AC untreated; **f** AC treated with 4.9% ozone for 2h; **g** GR untreated; **h** GR treated with 7.7% ozone for 2h. Bars, **a-f** 5 μ m; **g-h** 10 μ m

values of the C1s peaks of untreated and ozone-treated samples are shown in Table 3. GR with a well-developed polyaromatic structure showed the narrowest peak with a FWHM of 1.08 eV. The FWHM of C-1000 and AC were wider than that of GR. This means that C-1000 and AC had more disordered stacking planes and a less polyaromatic character than GR. It is suggested that C-400, with the broadest peak of 2.24 eV, has a completely amorphous structure composed of aliphatic carbons and small aromatic molecules.^{28,30}

The FWHM of the samples except GR increased after ozone treatment, which means that polyaromatic structures were destroyed by the ozone treatment. In particular, AC, with the broad peak of 2.13 eV, had quite a disordered structure due to the severe destruction of stacking planes by ozone treatment. On the other hand, no destruction of stacking planes on GR occurred after ozone treatment. As a result of XPS studies, it is suggested that the degree of development and orientation of stacking planes affects the resistance to oxidation by ozone treatment.

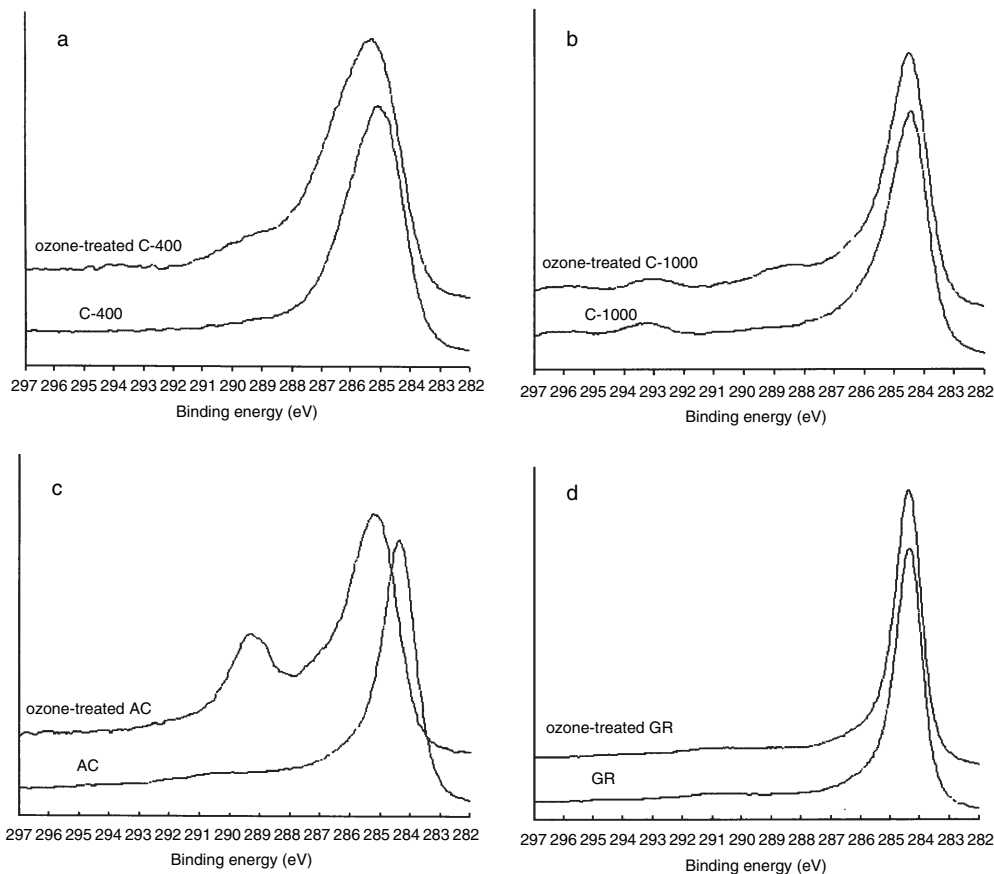
It is revealed that C-400 has an undeveloped polyaromatic structure, and is probably a complex of aliphatic carbons and small polyaromatic stacks cross-linked by ether and carboxyl groups and other oxygen-containing functional groups.^{31,32} It is suggested that oxidation to aliphatic carbon is much more independent than the cleavage of C=C bonding by ozone because the main component of C-400 is not aromatic layers. It is likely that a disordered

and rigid cross-linking structure impeded efficient reaction in all parts of the microstructure of C-400. Therefore, the surface chemical structure of C-400 was clearly changed after ozone treatment while neither weight loss nor change of surface morphology was observed.

The FWHM and O1s/C1s ratio of AC after ozone treatment increased remarkably, while only the O1s/C1s ratio increased conspicuously with C-1000. The microstructures of these samples are composed of stacking planes with random orientation.^{33,34} XPS revealed that the stacking planes of AC were more developed than those of C-1000 due to the removal of disorganized carbon during activation.³⁵ AC has a large relative surface area and a porous structure of high permeability due to activation. Thus, the oxidation reaction of AC occurred throughout the microstructure from the outer to the inner surface, while that of C-1000 took place mainly on the outer surface due to its undeveloped porous structure. Therefore, the outer surface of C-1000 was remarkably destroyed after ozone treatment as shown by SEM observation. It is suggested that the influence of ozone treatment differs in terms of the degree to which the stacking planes and porous structure are developed.

Potassium was detected by XPS on C-1000 but not on C-400, as depicted in Fig. 3, even though the samples are derived from the same original sawdust. During carbonization, carbon, oxygen, and hydrogen are released from charcoal, which raises the relative ratio of ash content with increasing carbonizing temperature. It is suggested that

Fig. 3a–d. X-ray photoelectron spectra of the samples treated and untreated with ozone under the same conditions as for SEM (Fig. 2). **a** C-400, **b** C-1000, **c** AC, **d** GR



potassium was not detected by XPS due to the low relative ratio of potassium against carbon in C-400 in the early stage of carbonization. On the other hand, because the relative ratio of potassium against carbon in C-1000 was higher than that in C-400 due to the high carbonization temperature (1000°C), the potassium peak was detected by XPS. Furthermore, the detection sensitivity for potassium by XPS is different depending on the state of the potassium. The peak for potassium oxide is more detectable than that of potassium carbonate.³⁶ For C-1000, it is likely that the potassium peak was detected by XPS due to the accumulation of potassium oxide on the carbon surface during carbonization. As is commonly known, potassium compounds such as a potassium hydroxide catalyze the oxidation of carbon materials. Therefore, it is suggested that potassium compounds in C-1000 catalyzed the oxidation, and accelerated the destruction of the carbon structure. Consequently, the weight loss and the destruction on the surface of the cell wall of C-1000 by ozone treatment occurred to remarkable extents, and were comparable with those of AC.

Rate constant and assumption of half-life

Rate constants of the decline of charcoal were calculated based on the weight decrease of C-1000 and AC in the range in which a prompt decrease in weight or sample burning was not induced (Table 4). The rate constants for C-1000 were lower than those of AC.

For C-400 and GR, the rate constants were not estimated because no decrease in weight was observed (Fig. 1). The exponential curve was fitted to the plot of the rate constants to the ozone concentration by assuming that the rate constant was zero at 0% ozone (Fig. 4). The resulting equation of the exponential curve was the following:

$$\alpha = 0.95857 \times 10^{-5} \times (\exp(C \times 0.93838) - 1) \quad (2)$$

where α : rate constant (min^{-1})
C: ozone concentration (%)

The half-life of C-1000 with ozone in air was roughly estimated. The rate constant was calculated using Eq. 2 with 29ppb ozone in air, which is a mean value at the forest floor.³⁷ It has been reported that the application of charcoal on the forest floor of a leguminous tree, *Acacia mangium*,

enhanced nodule formation on the root.³⁸ Its half-life was estimated to be 5.1×10^4 years (Table 5). The half-life of AC was calculated to be 1.4×10^3 years. C-400 was much more stable against ozone than C-1000 (Fig. 1). Thus, it is suggested that the half-life of C-400 with ozone in air is of geological length and that charcoal carbonized at a lower temperature is more stable against ozone. This is consistent with the geological research on charcoal.³⁹

Conclusions

We obtained the results from this study as follows:

1. The weight of C-1000 and AC was significantly decreased by ozone treatment although no such decrease was observed in C-400 and GR.
2. Change of the surface morphology was observed in the ozone-treated C-1000 and AC.
3. There was no correlation between the weight decrease of the samples and the contents of carbon, hydrogen, and oxygen.
4. Stability of the samples against ozone depended on the development of hexagonal carbon layers.
5. The half-life of C-1000 with ozone in air was estimated to be 5.1×10^4 years.

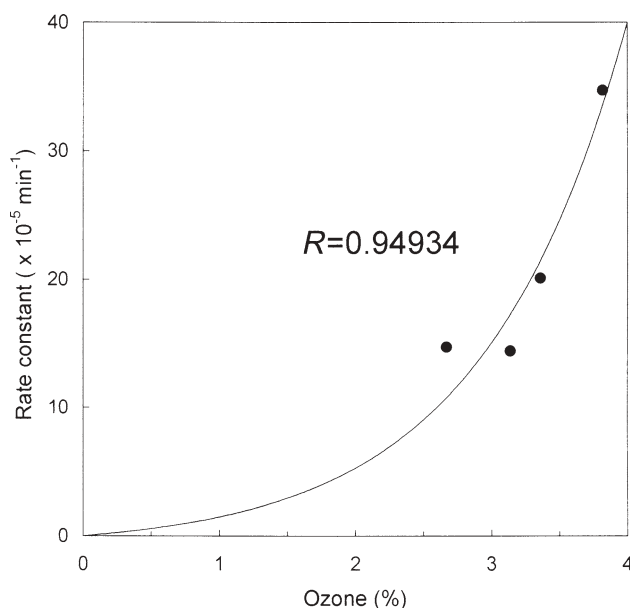


Fig. 4. Plot of the rate constants versus the ozone concentrations at which C-1000 was treated for 4h

Table 4. Rate constants ($\times 10^{-5}/\text{min}$) of the weight decrease at each ozone concentration

Ozone concentration (v/v %)	C-1000	AC	C-400	GR
8.46	–	–	0.00	–
8.13	–	–	–	–
7.07	–	503	–	–
4.94	–	300	–	–
3.82	34.7	–	–	–
3.36	20.1	–	–	–
3.14	14.4	–	–	–
2.89	–	101	–	–
2.67	14.7	–	–	–

Table 5. Rate constants of the weight decrease of C-1000 and AC and the estimated half-life at 29ppb ozone

Sample	Rate constant (min^{-1})	Half-life (years)
C-1000	2.61×10^{-11}	5.1×10^4
AC	9.53×10^{-10}	1.4×10^3

The charcoal made by carbonization at lower temperatures has an economic advantage in that it is less costly than the charcoal made at higher temperatures. Thus, the charcoal made at lower temperatures is more suitable for carbon sequestration by its utilization for soil amendment and for forestation and carbonization projects in developing countries, as proposed by Okimori et al.⁴

Acknowledgments Part of this study was carried out at the Uji Branch of the Research Institute of Innovative Technology for the Earth (RITE), and was supported by a Grant-in-Aid from the New Energy and Industrial Technology Development Organization (NEDO) and a Grant-in-Aid for Scientific Research (14002121) from the Ministry of Education, Culture, Sports, Science, and Technology of Japan. We are much obliged to Mr. Nobuo Ishizaki for his kind advice and suggestions.

References

- Houghton JT, Meira Filho LG, Callander BA, Harris N, Kattenberg A, Maskell K (eds) (1996) Climate change 1995. The science of climate change. Contribution of working group I to the second assessment report of the Intergovernmental Panel on Climate Change. Cambridge University Press, Cambridge
- Seifritz W (1993) Should we store carbon in charcoal? *Int J Hydrogen Energ* 18:405–407
- Glaser B, Lehmann J, Zech W (2002) Ameliorating physical and chemical properties of highly weathered soils in the tropics with charcoal – a review. *Biol Fertil Soils* 35:219–230
- Okimori Y, Ogawa M, Takahashi F (2003) Potential of CO₂ emission reductions by carbonizing biomass waste from industrial tree plantation in South Sumatra, Indonesia. *Mit Adap Strat Gl Change* 8:261–280
- Ogawa M (1994) Symbiosis of people and nature in the tropics. *Farm Jap* 28:10–34
- Kawamoto K, Kurusu T, Ahmad S, Al-Hajeri MF, Al-Harbi AH (2003) Effect of symbiotic microorganisms and partial hydroponics on the growth of tree seedlings under arid conditions. *J Arid Land Studies* 12:195–201
- Yatagai M, Ito R, Ohira T, Oba K (1995) Effect of charcoal on purification of wastewater. *Mokuzai Gakkaishi* 41:425–432
- Pulido LL, Ishihara S, Imamura Y, Hata T (1996) Research and development of carbon composites from wood charcoal for environmental clean-up and their applications. *Wood Res* 83:43–46
- Matsumoto S (1999) Fundamentals and practices of soil bioremediation. *Soil Sci Plant Nutr* 45:237–251
- Oya A, Iu WG (2002) Deodorization performance of charcoal particles loaded with orthophosphoric acid against ammonia and trimethylamine. *Carbon* 40:1391–1399
- Yasuda E, Suzuki Y, Inoue Y, Izawa H, Ebato O, Takano S, Kihara K, Kondou A, Ookawa M, Hiraoka T, Shimada M, Kume M, Niya K, Aiba Y, Takeuchi K (1995) Microstructural change of pitch-derived carbon matrix in C/C composite by ozone treatment on carbon fiber (in Japanese). *TANSO* 170:247–254
- Sutherland I, Sheng E, Bradley RH, Freakley PK (1996) Effects of ozone oxidation on carbon black surfaces. *J Mater Sci* 31:5651–5655
- Sharypov VI, Kuznetsov BN, Baryshnikov SV, Beregovtsova NG, Selyutin GE, Chumakov VG, Kamianov VF (1999) Some features of chemical composition, structure, and reactive ability of Kansk–Achinsk lignite modified by ozone treatment. *Fuel* 78:663–666
- Zhou J, Wipf DO (2001) UV/ozone pretreatment of glassy carbon electrodes. *J Electroanal Chem* 499:121–128
- Mawhinney DB, Yates JT Jr (2001) FTIR study of the oxidation of amorphous carbon by ozone at 300K – direct COOH formation. *Carbon* 39:1167–1173
- Kung S-C, Hwang KC, Lin IN (2002) Oxygen and ozone oxidation-enhanced field emission of carbon nanotubes. *Appl Phys Lett* 80:4819–4821
- Takagaki T, Sugiura T (1976) About the ozone removal by activated charcoal (in Japanese). *Kogai To Taisaku* 12:306–314
- Ishizaki N (1990) Ozone-degradation material – KF filter for ozone degradation (in Japanese). In: *Ozone Bunkai Gijutsu*. Sanyusyobo, Yokohama, pp 145–154
- Nakayama S (1990) Technique for treatment of waste ozone – activated charcoal (in Japanese). In: *Ozone Bunkai Gijutsu*. Sanyusyobo, Yokohama, pp 195–200
- Arai K (1993) Honeycomb filter for ozone degradation (in Japanese). *Gekkan Food Chemical* 3:41–46
- Nakayama M, Sanada Y (1993) Modification of pyrolytic graphite surface with plasma irradiation. *J Mater Sci* 28:1327–1333
- Yue ZR, Jiang W, Wang L, Gardner SD, Pittman CU Jr (1999) Surface characterization of electrochemically oxidized carbon fibers. *Carbon* 37:1785–1796
- Darmstadt H, Roy C, Kaliaguine S (1994) ESCA characterization of commercial carbon blacks and of carbon blacks from vacuum pyrolysis of used tires. *Carbon* 32:1399–1406
- Clark DT, Thomas HR (1976) Applications of ESCA to polymer chemistry X. Core and valence energy levels of a series of polyacrylates. *J Polym Sci, Polym Chem Ed* 14:1671–1700
- Proctor A, Sherwood PMA (1982) X-ray photoelectron spectroscopic studies of carbon fibre surfaces. 1. Carbon fibre spectra and the effects of heat treatment. *J Electron Spectrosc Relat Phenom* 27:39–56
- Lee YS, Lee BK (2002) Surface properties of oxyfluorinated PAN-based carbon fibers. *Carbon* 40:2461–2468
- Wang JG, Guo QG, Liu L, Song JR (2002) Study on the microstructural evolution of high temperature adhesives for graphite bonding. *Carbon* 40:2447–2452
- Takahagi T, Ishitani A (1988) XPS study on the surface structure of carbon fibers using chemical modification and C1s line shape analysis. *Carbon* 26:389–396
- Darmstadt H, Roy C, Kaliaguine S, Choi SJ, Ryoo R (2002) Surface chemistry of ordered mesoporous carbons. *Carbon* 40:2673–2683
- Nishimiya K, Hata T, Imamura Y, Ishihara S (1998) Analysis of chemical structure of wood charcoal by X-ray photoelectron spectroscopy. *J Wood Sci* 44:56–61
- Oberlin A, Villey M, Combaz A (1980) Influence of elemental composition on carbonization. Pyrolysis of kerosene shale and kuckersite. *Carbon* 18:347–353
- Villegas JP, Duran-Valle CJ, Valenzuela-Calahorra C, Gomez-Serrano V (1998) Organic chemical structure and structural shrinkage of chars prepared from rockrose. *Carbon* 36:1251–1256
- Innes RW, Fryer JR, Stoeckli HF (1989) On the correlation between micropore distribution obtained from molecular probes and from high resolution electron microscopy. *Carbon* 27:71–76
- Ishimaru K, Vystavel T, Bronsveld P, Hata T, Imamura Y, Hosson JD (2001) Diamond and pore structure observed in wood charcoal. *J Wood Sci* 47:414–416
- Gonzalez MT, Rodriguez-Reinoso F, Garcia AN, Marcilla A (1997) CO₂ activation of olive stones carbonized under different experimental conditions. *Carbon* 35:159–165
- Yokoyama S, Tanaka K, Toyoshima I, Miyahara K, Yoshida K, Tashiro J (1980) X-ray photoelectron spectroscopic study of the surface of carbon doped with potassium carbonate. *Chem Lett* 5:599–602
- Takenaka C, Hibino M, Kuriyama H (2001) Measurements of ozone vertical distribution in a hinoki (*Chamaecyparis obtusa*) forest using a sensitive ozone passive sampler. *Nagoya Univ For Sci* 20:1–6
- Yamato M, Supriyo H (2002) The effect of charcoal application on *Acacia mangium*. In: Proceedings of the seminar on Dipterocarp reforestation to restore environment through carbon sequestration, September 26–27, 2001, Yogyakarta, Indonesia, pp 159–163
- Cowling RM, Cartwright CR, Parkington JE, Allsopp JC (1999) Fossil wood charcoal assemblages from Elands Bay Cave, South Africa: implications for Late Quaternary vegetation and climates in the winter-rainfall fynbos biome. *J Biogeogr* 26:367–378